Cathode Exhaust Gas Recirculation

For Polymer Electrolyte Fuel Cell Stack

F. Becker[1,*], F. Pillath[1], J. Kallo[2]

[1] German Aerospace Center (DLR e.V.), Institute of Engineering Thermodynamics,

Hein-Saß-Weg 22, D-21129 Hamburg, Germany

[2] German Aerospace Center (DLR e.V.), Institute of Engineering Thermodynamics,

Pfaffenwaldring 38, D-70569 Stuttgart, Germany

[*] Corresponding author: Florian.Becker@dlr.de

Abstract

To ensure the required reliability and efficiency of a Polymer Electrolyte Fuel Cell (PEFC) system, an emergency situation in which the supply of ambient air has to be sealed off, is considered. In this case oxygen from a separate gas tank is fed to the fuel cell system.

To prevent the loss of oxygen by the exhaust, the cathode gas can be fed back by cathode gas recirculation while oxygen is injected. Thereby the opportunity to feed back the humidity of the exhaust air for additional fuel cell humidification becomes available.

The humidification of a PEFC is essential to ensure high protonic conductivity and reduce voltage losses. However, the water content of the inlet gas has to be regulated to prevent the electrodes from flooding. To control the humidity of the system the gas flow rate, the temperature of the fuel cell and the cathode gas can be adjusted. In addition, the enhanced water content in the system allows increasing the operating temperatures.

This work focuses on an experimental study of a 12 kW PEFC-System with cathode gas recirculation and a phenomenological model to optimize the fuel cell humidification depending on the operating parameters.

Keywords: Polymer Electrolyte Fuel Cell, (PEFC), Cathode Gas Rrecirculation, Humidification, Membrane Resistance, Fuel Cell Oxygen Supply, Phenomenological Model

1 Introduction

Effective and reliable operation of low temperature polymer electrolyte fuel cells (LT-PEFC) requires an optimized thermal- and water management of the fuel cell system. The performance and efficiency of the fuel cell system can be optimized by adjustment of the operating parameters (flow rate, stoichiometric ratio, oxygen concentration, operating pressure and stack temperature).

As extensively discussed in [1-2], the polymer electrolyte membranes have to be adequately humidified to assure the required reliability of a PEFC. Dehydration of the membrane leads to a decreasing proton conductivity and thus to a low fuel cell performance due to increased ohmic losses [3]. Furthermore, the dehydration will lead to membrane degradation [4].

When the cathode gas is oversaturated with water, steam condenses inside the cathode and blocks the gas supply channels of the flow fields, which leads to a starvation of oxygen at the active catalyst surface. The occurring concentration loss reduces the PEFC performance whereas carbon corrosion of the gas diffusion layers occurs [5].

To reduce the complexity of the fuel cell system and its volume, it is possible to renounce humidification systems, whereby the fuel cells performance is decreased [6].

Furthermore, LT-PEFC systems are not operational if the used air is highly contaminated with harmful gases or particles, which could lead to a catalyst reduction or to a blockage of the gas diffusion layers. In some situations like aircraft applications the fuel cell must be able to operate even in an emergency case in which the supply of oxidant from the ambient air has to be sealed off. In this case oxygen from a separate gas tank is fed to the fuel cell system to keep the oxygen concentration constant at the cathode inlet. To carry out the product water a stoichiometric ratio of 1.2 to 1.3 is required, which implies an excess of oxygen [7].

To prevent the loss of unused oxygen by the exhaust, the cathode gas can be fed back into the fuel cell by cathode gas recirculation while oxygen is injected. Thereby the opportunity to feed back the humidity and heat of the exhaust air for additional fuel cell humidification becomes available. The cathode humidification by partial exhaust gas recirculation for PEM fuel cell was studied by [8], where the advantages of humidification by exhaust gas recirculation can be regarded as a good alternative.

The water content of the inlet gas has to be regulated to prevent the electrodes from flooding and to enable the access of oxygen. To control the humidity of the system the gas flow rate, the temperature of the fuel cell stack and the temperature of the condenser can be adjusted. Thereby a relative humidity at the cathode outlet of about 100 % is required [3, 9, and 10].

This work focuses on experimental study of a 12 kW PEFC-System with closed cathode gas recirculation as well as a phenomenological model to optimize the fuel cell humidification depending on the operating parameters. The theoretical analysis shows the correlation of the operation parameters and the relative humidity at the cathode outlet. Whereby the experimental results show an enhancement of the fuel cells performance by increasing of the condenser and stack temperatures regarding the optimization of the water and thermal management. Finally, an outlook on arising prospects of this concept is given.

2 System description

The used 12 kW PEM fuel cell system (Hydrogenics - HyPM XR 12) consists of 60 cells with a total active surface of 496 cm^2. According to [11], the cells include multi-meander flow fields and a Nafion® membrane with a catalyst load of 0.3 mg Pt cm^{-2}. The PEMFC system achieves a rated power of 12 kW, a maximal output current of 350 A and an output voltage range of 30-60 V. Furthermore the system blower was substituted by a side channel blower which is able to operate with humid gases (Gardner Denver - G-BH7). Figure 1 shows the

schematic setup of the cathode gas recirculation system. In the Appendix the principle process scheme including the PEMFC system and listed subcomponents are shown.

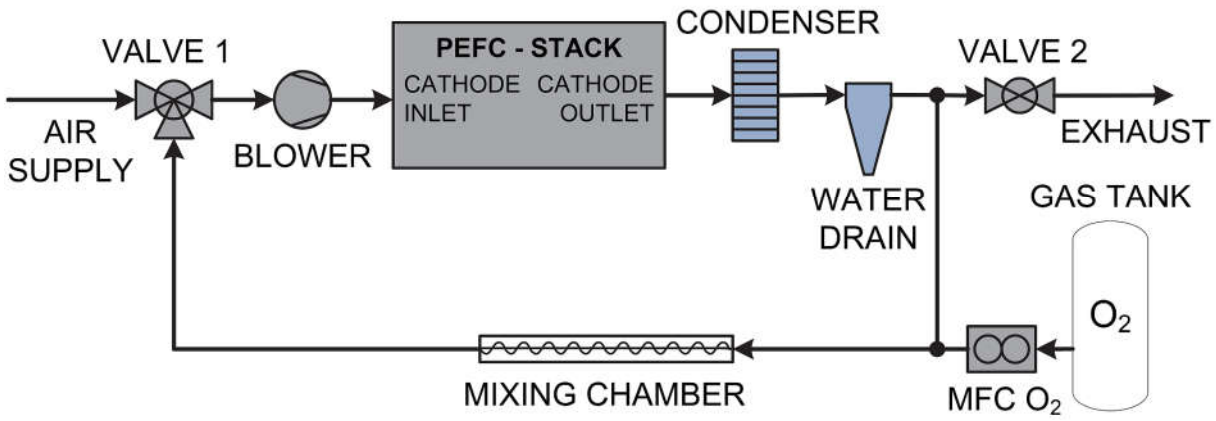

Fig. 1: Principle process scheme of cathode gas recirculation.

In this configuration, it is possible to provide the required cathode gas in open operation from the ambient air. After switching the two valves at the in- and outlet of the cathode, the system operates in closed loop configuration. Thereby an oxygen mass flow controller replaces the consumed oxygen in the exhaust gas from a separate gas tank in dependence of the measured stack current. To prevent a continuous increase or decrease of the oxygen content due to the tolerance of the oxygen mass flow controller or the current measurement, the oxygen concentration at the cathode inlet is measured. Thus a possible deviation of the oxygen concentration will be counteracted by the mass flow controller. For the experimentation the stack current, stack temperature, condenser temperature, oxygen concentration and the flow rate can be adjusted. Whereas the controlled stack temperature corresponds to the measured temperature of the coolant outlet.

3 Calculations, Simulations and Experiments

This section describes the theoretical analysis and experiments accomplished to characterize the impact of operating parameters in closed loop configuration on the cathode gas condition and the performance of a PEMFC system.

3.1 Theoretical Analysis

For the theoretical analysis the following assumptions are considered:

(i) Steady state of the system

(ii) Every gas is assumed to be an ideal gas

(iii) Water diffusion from cathode to anode and vice versa are neglected

(iv) Diffusion of oxygen and nitrogen from cathode to anode is neglected

(v) Constant cathode pressure of 101325 Pa

(vi) Adiabatic processes

(vii) Temperature variation due to injected oxygen and blower friction is neglected

The theoretical analysis is focused on the influence of the operation parameters (stack temperature, operating pressure, cathodic stoichiometric ratio and oxygen concentration) on the relative humidity of the cathode gas, which has a major impact on the efficiency and durability of the PEMFC.

According to [10] the relative humidity of the cathodic exhaust gas ($rh_{cath.out}$) in open configuration can be calculated using Eq. (1), whereas the saturation vapor pressure of water can be taken from IAWPS-95 [12].

$$rh_{\text{cath.out}} = 2\, p_{\text{cath.}}\, p_{\text{s}(T_{\text{FC}})}^{-1}\, (\lambda\, F_{\text{O2\_cath.in}}^{-1} + 1)^{-1}\, 100\% \qquad (1)$$

Here the relative humidity of the cathodic inlet air is assumed to be zero (if applicable). In closed loop configuration the warm and humid exhaust gas is fed back to the cathodic inlet.

Thus, to calculate the relative humidity for the closed loop configuration some further iterative calculations are required.

To determine the cathodic gas conditions depending on the mode of operation a numerical model was built via MATLAB/Simulink®. The molar flow rates of every gas component (n_i) at the cathode inlet of the fuel cell depending on the substance amount fractions (x_i) are calculated by the Eq. (2) – (5).

$$n_{O2\_cath.in} = I \ \lambda \ Z \ 4^{-1} \ F^{-1} \qquad (2)$$

$$n_{cath.in} = n_{O2\_cath.in} \ x_{O2\_cath.in}^{-1} \qquad (3)$$

$$n_{N2\_cath.in} = n_{cath.in} \ x_{N2\_cath.in} \qquad (4)$$

$$n_{H2O\_cath.in} = n_{cath.in} \ x_{H2O\_cath.in} \qquad (5)$$

The molar flow rates of the cathodic exhaust gas and its components are calculated by the Eq. (6) – (9)

$$n_{O2\_cath.out} = I \ (\lambda - 1) \ Z \ 4^{-1} \ F^{-1} \qquad (6)$$

$$n_{H2O\_cath.out} = n_{H2O\_cath.in} + (I \ Z \ 2^{-1} \ F^{-1}) \qquad (7)$$

$$n_{N2\_cath.out} = n_{N2\_cath.in} \qquad (8)$$

$$n_{cath.out} = \sum n_{i\_cath.out} \quad \text{where i} = O_2; N_2; H_2O \qquad (9)$$

At this point it cannot be said, which part of the water is gaseous or liquid. Hence, the temperature dependent saturation vapor pressure is used to calculate the relative humidity in Eq. (11) by comparison of the saturation vapor pressure with the partial pressure of water $p_{H2O\_cath.out}$ in Eq. (10).

$$p_{H2O\_cath.out} = p_{cath.out} \ n_{H2O\_cath.out} \ n_{cath.out}^{-1} \qquad (10)$$

With:

$p_{H2O\_cath.out} \geq p_{s(TFC)}$: $p_{H2O\_cath.out} = p_{s(TFC)}$

$p_{H2O\_cath.out} < p_{s(TFC)}$: $p_{H2O\_cath.out} = p_{cath.out} \ n_{H2O\_cath.out} \ n_{cath.out}^{-1}$

$$rh_{cath.out} = p_{H2O\_cath.out} \ p_{s(TFC)}^{-1} \ 100\% \qquad (11)$$

As shown in Figure 1, a condenser is placed after the cathode outlet. Thereby the opportunity is given to adapt the temperature ($T_{cond.}$) and accordingly the relative humidity of the exhaust gas ($rh_{cath.out}$), which is fed back to the cathode inlet. Due to mass conservation (Eq. (10) and (11)) can be used to calculate the relative humidity at the condenser outlet by Eq. (12).

$$rh_{cond.out} = p_{H2O\_comd.out} \; p_{s(Tcomd.out)}^{-1} \; 100\% \qquad (12)$$

To remove the liquid water downstream the condenser a water drain is implemented as well. The molar flow rates of the remaining water vapor ($n_{H2O(v)\_cond.out}$) and the removed water ($n_{H2O(l)\_cath.out}$) are calculated by Eq. (13) and (14).

$$n_{H2O(v)\_cond.out} = (n_{O2\_cath.out} + n_{N2\_cath.out}) \; (p_{cond.out} \; p_{H2O\_cath.out}^{-1} - 1)^{-1} \qquad (13)$$

$$n_{H2O(l)\_cond.out} = n_{H2O\_cath.out} - n_{H2O(v)\_cond.out} \qquad (14)$$

To complete the initial calculation, the substance amount fractions of the recycled gas at the cathode inlet (x_i) have to be determined (Eq. (16)). Therefore, the molar flow rate of the injected oxygen ($n_{O2\_inj.}$) has to be taken into account (Eq. (15)).

$$n_{O2\_inj.} = I \; Z \; 4^{-1} \; F^{-1}) \qquad (15)$$

$$x_{i\_cath.in} = n_{i\_cath.in} \; (\sum n_{i\_cath.out} - n_{H2O(l)\_cond.out} + n_{O2\_inj.})^{-1} \quad \text{where i} = O_2; N_2; H_2O(v) \qquad (16)$$

For the further iterations the calculated values are set into Eq. (3) – (5). According to the assumptions (v), (vi) and (vii) the pressure at the cathode inlet is constant (101325 Pa) and the temperature at the cathode inlet equals to the condensation temperature.

During the experimentation, the pressure and the temperature of the cathode gas depend on the mode of operation, the position of measurement and also on the test-setup. If they are known, the measured parameters can be used to optimize the model and calculate the relative humidity at e.g. the cathode inlet of the fuel cell.

3.2 Experiments

In this study the cathodic standard flow rate (v_0) is set with respect to Eq. (17). The use of the standard flow rate ensures that temperature, pressure and humidity during the operation do not

affect the total cathodic flows. However, these parameters are taken into account by the calculation of the controlled oxygen concentration (C_{O2}) in Eq. (18), where the measured values of the operating pressure, temperature and relative humidity at the cathode inlet are considered.

$$v_0 = I\ \lambda\ Z\ R\ T_0\ 100\%\ 4^{-1}\ F^{-1}\ p_0^{-1}\ C_{O2}^{-1} \qquad (17)$$

$$C_{O2} = (p_{abs} - p_s(T)\ rh\ 100\%^{-1})\ F_{O2}\ p_{abs}^{-1}\ 100\ \% \qquad (18)$$

4 Results an discussions

Contours of the relative humidity at the cathode outlet in dependency of the stoichiometric ratio and the fuel cells temperature in closed loop configuration are shown in Figure 2. The stoichiometric ratio is determined by the cathodic flow rate according to Eq. (17). The oxygen concentration at the cathode inlet equals 20.9 % and the corresponding condensation temperature is 15°C. Due to the assumptions (v) and (vi) the condensation temperature equals to the temperature at the cathode inlet, if the cathodic gas is recirculated.

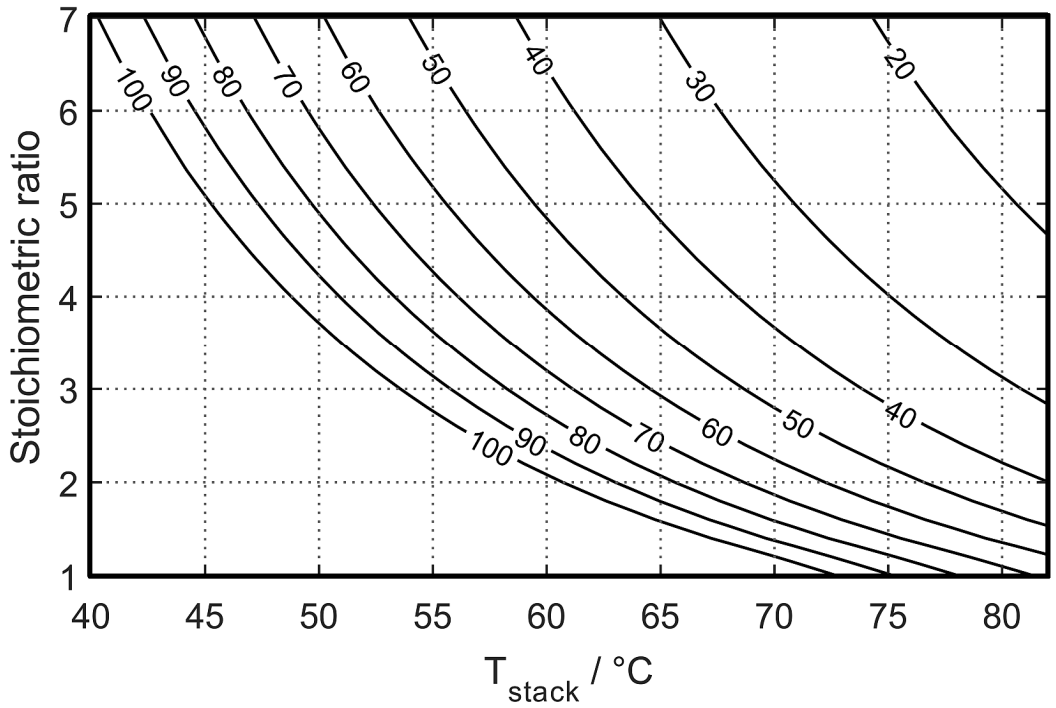

Fig. 2: Calculated contours of the relative humidity at the cathode outlet in dependency of the stoichiometric ratio and the fuel cells temperature in closed loop configuration;
$T_{cond.} = T_{cath.in} = 15°C$

In Figure 2 it can be seen, how the relative humidity will decrease, when the stack temperature is raised and the stoichiometric ratio is increased by the volume flow. The saturation vapor pressure of the cathode gas increases at higher temperatures. Therefore, the relative humidity will decrease according to Eq. (11). When the volume flow rate becomes higher, the partial pressure of water and the relative humidity go down since the flow rate of product water does not change.

In a steady-state condition the injected oxygen flow rate does not depend on the stoichiometric ratio. Thus, the relative humidity is not affected, if the stoichiometric ratio is changed by variation of the oxygen concentration of the cathode air at constant total flow rate.

Figure 3 illustrates the correlation between the stack temperature, the condensation temperature and the relative humidity at the cathode outlet of the fuel cell.

Figure 3a) shows the contours of the relative humidity at a total flow rate which corresponds to a stoichiometric ratio of 2.0 and to a stoichiometric ratio of 2.5 (recommended by the fuel cells manufacturer) in Figure 3b). The oxygen concentration at the cathode inlet in both cases is 20.9 %. By comparison of the contours it can be seen, that the relative humidity decreases with the increase of the stoichiometric ratio due to the higher flow rate as mentioned above. Furthermore, the condensation temperature controls the relative humidity downstream the condenser and hence the cathode inlet.

The maximum relative humidity at the cathode in- and outlet of the fuel cell can be reached, without active cooling of the condenser. However, the condensation temperature as well as the stack temperature have to be adjusted to prevent the cells from flooding and to optimize the water management of the fuel cell system.

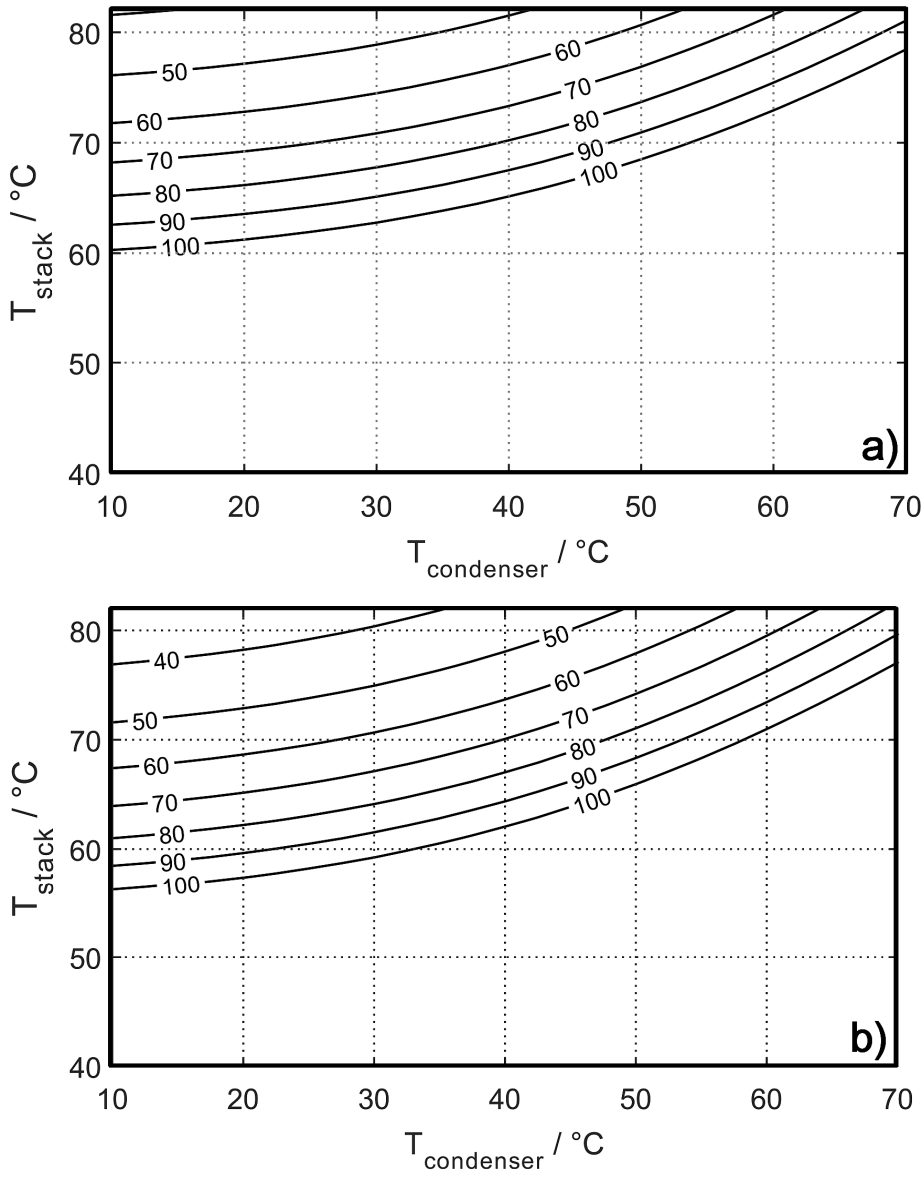

Fig. 3: Calculated contours of the relative humidity at the cathode outlet with respect to the stack temperature and the condensation temperature in closed loop configuration; λ = 2.0 (a) λ = 2.5 (b)

During the experiment, measurements were carried out to optimize the performance of the fuel cell system. The system blower provides the required cathodic volume flow, which results in parasitic losses. Figure 4 shows the correlation of the provided stack power and the needed power of the used blower.

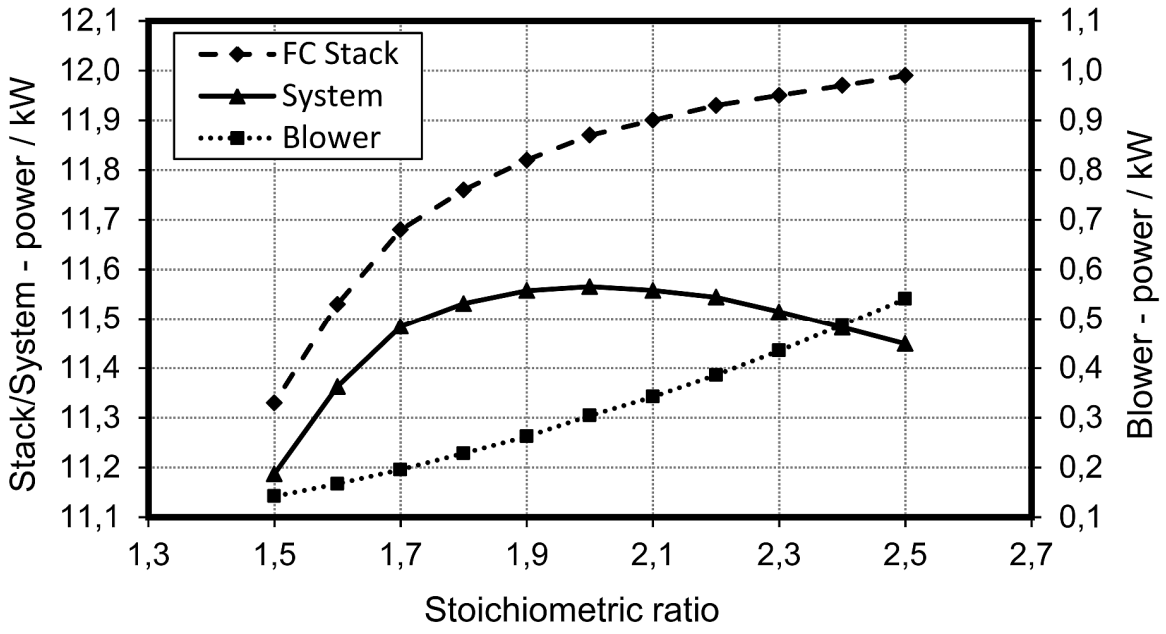

Fig. 4: Comparison between the provided electrical power of the fuel cell stack and the parasitic loss of the blower. Fuel Cell: *HyPM XR-12*; Blower: *Gardner Denver 2BH7 610-0A*. I = 300 A; T_{stack} = 62°C; $T_{cond.}$ = 15°C.

The maximum measured stack power was achieved at a stoichiometric ratio of 2.5 as recommended by the fuel cells manufacturer. Anyway the provided system power regarding the parasitic loss of the blower reached its maximum at a stoichiometric ratio of 2.0. Therefore, a stoichiometric ratio of 2.0 was used for the further experiments.

To determine the influence of the stack and condensation temperature on the performance of the fuel cell, first the condensation temperature was increased stepwise at a certain load (I = 300 A). Figure 5a shows the measured values of the maximum, average and minimum cell voltage, as well as the stack voltage with respect to the time. The measured operating temperatures and the relative humidity at the cathode inlet are shown in Figure 5b.

As the temperature of the condenser is raised, the stack- and cell voltages decrease. This voltage drop arises due to the reduction of the active cell area by a gradual flooding of the cells. The correlation of the higher relative humidity of the recirculated cathode gas and the rising temperature of the condenser can also be seen.

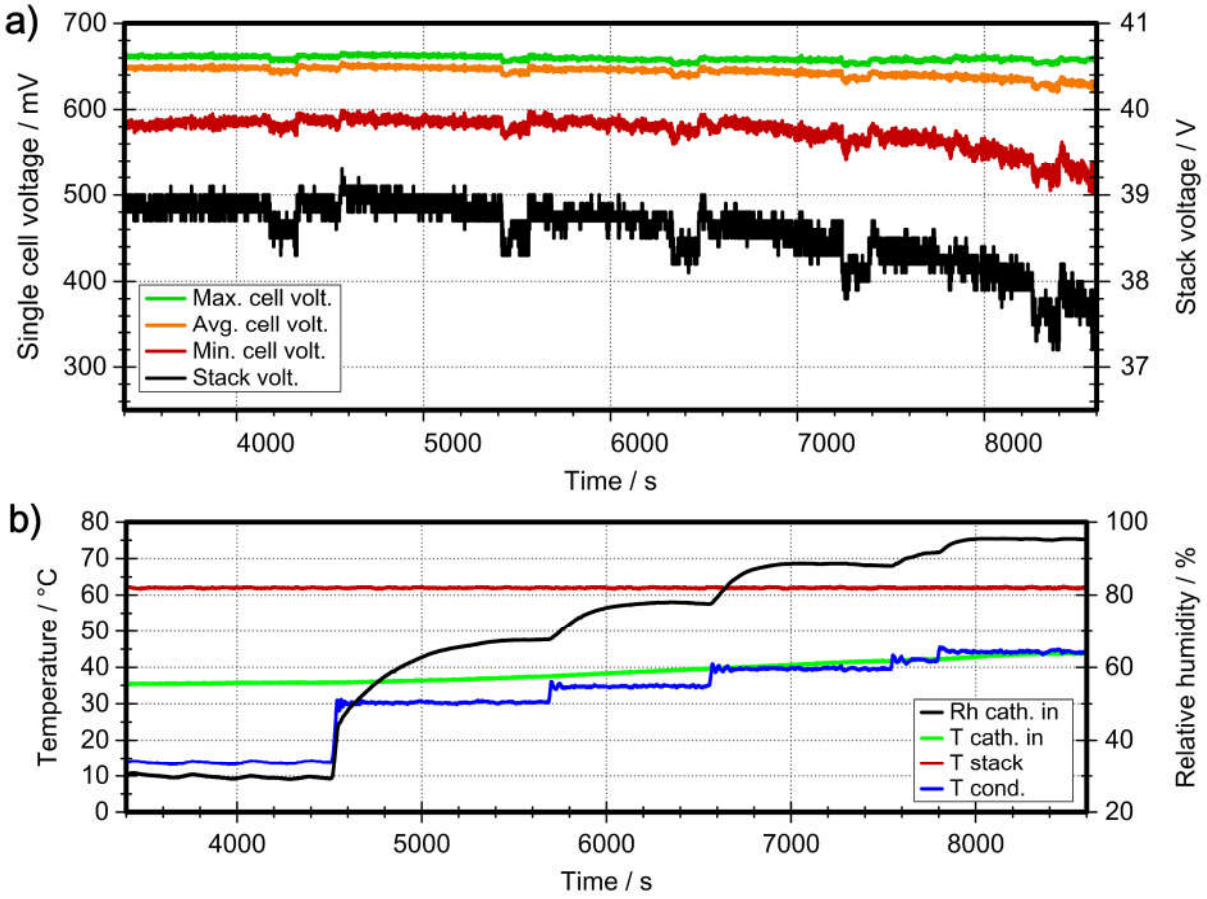

Fig. 5: Measured cell - and stack voltages (a) operating temperatures and relative humidity at the cathode inlet of the fuel cell at different condensation temperatures (b). T_{stack} = 62°C, λ = 2.0; I = 300 A (+ 5 A during impedance measurements)

To determine the impact of the additional entry of moisture on the membrane resistance, an impedance measurement was conducted prior to any increase in the condensing temperature. Therefore, an impedance spectroscope (Zahner Zennium IM6) was used. During the impedance measurements an additional 5 A DC load superimposed by an AC load (current amplitude = 3.8 A; frequency range = 100 MHz...10 kHz) was applied to the stack. The associated voltage dips due to the additional load can be seen in Figure 5a.

During the impedance measurements the resulting cell voltages at 17 cells, distributed over the stack, were recorded to determine the corresponding membrane resistances. Figure 6 shows the results of the measurement and the distribution of the measuring positions. The Cell number 1 indicates the first cell of the stack, where the fuel cells manifold including gas/coolant in- and outlets is located.

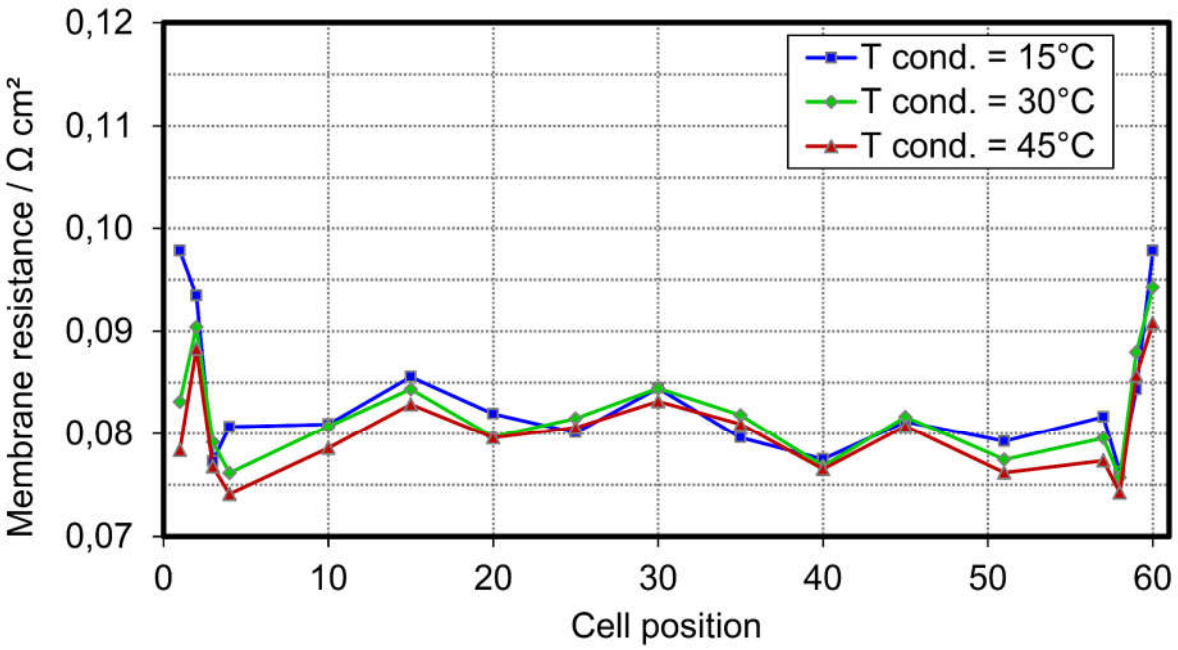

Fig. 6: Membrane resistances distributed over the stack at different temperatures of the condenser (T_{stack} = 62°C, λ = 2.0, I = 305 A).

In the front and rear area of the stack, higher membrane resistances were measured. This relates to the humidity and temperature distribution in the stack. The proton conductivity increases with a higher water content of the membrane and thus with the humidification of the cathode gas. As the condensing temperature in closed loop configuration is raised, more humidity and heat is feed back to the cathode. In Figure 6 it can be seen, that the membrane resistance especially at the front side of the stack decreases, as the condenser temperature is raised.

According to the model, the cathode exhaust gas will be saturated in the considered operating points. If the membranes are fully hydrated, the membrane resistance will not decrease further by additional humidification. Therefore, just a slight decrease of the membrane resistances can be noticed within the measurements in Figure 6.

Despite the identified reduction of membrane resistance with increasing condensation temperature, the measured voltages decrease by gradual flooding of the cells as described above. To prevent the cells from flooding, the stack temperature was increased stepwise from

62°C to 72.5°C in the experimentation. Figure 7 illustrates the measured voltages as well as the operating temperatures and the humidity at the cathode inlet.

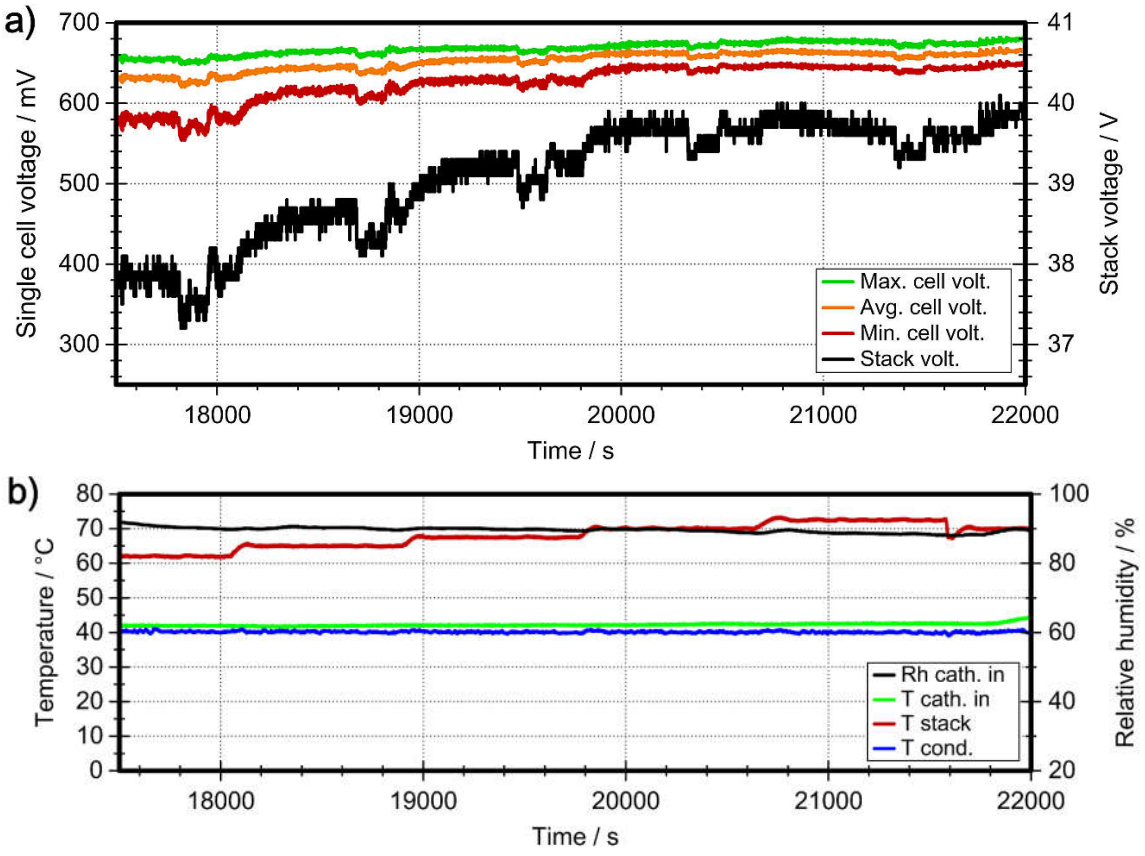

Fig. 7: Measured cell - and stack voltages (a), operating temperatures and relative humidity at the cathode inlet of the fuel cell at variation of the stack temperature (b). $T_{cond.}$ = 40°C, λ = 2.0, I = 300 A (+ 5 A during impedance measurements)

With increase of the stack temperature, the stack and cell voltages increase as expected. Due to the decreasing relative humidity of the cathode exhaust air, the flooding of the cells is counteracted. At an operating temperature of 72.5°C a voltage drop can be seen due to a gradual dehydration of the cells. To verify this, the relative humidity at the cathode in- and outlet of the fuel cell was calculated and compared to the measurements. Table 1 demonstrates the relative humidity at varying stack temperatures and proves the correlation of the calculation (c) and measuring points (m) from the experiments.

The results of the corresponding impedance measurements are shown in Figure 8, where the membrane resistances are illustrated for the different operating temperatures.

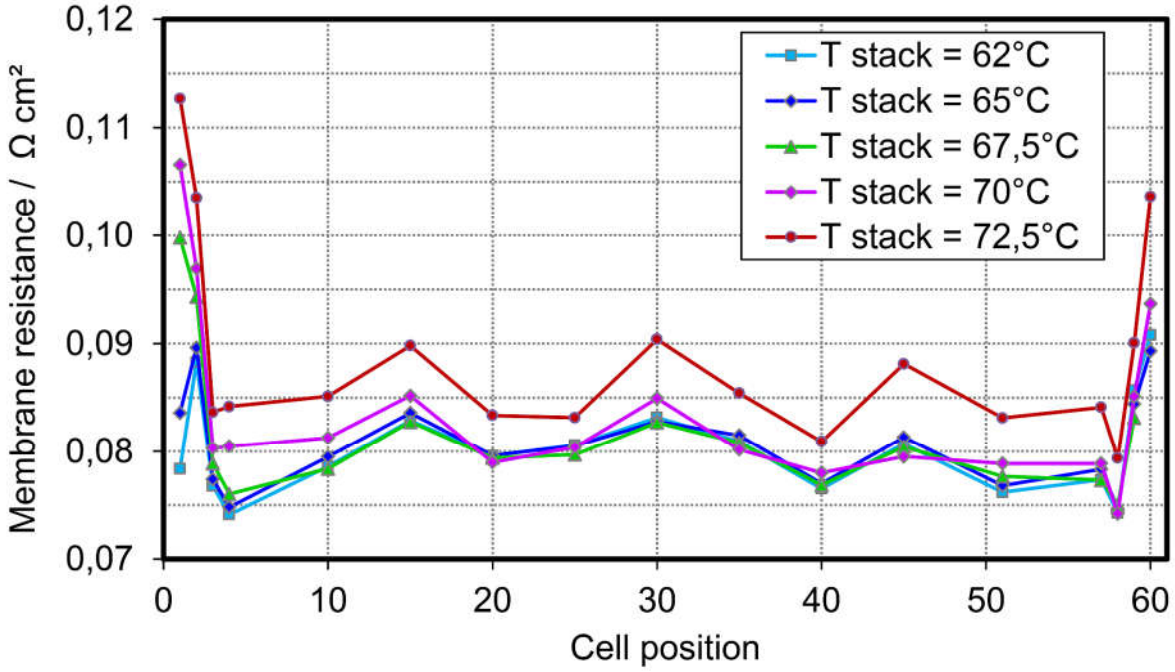

Fig. 8: Membrane resistances distributed along the stack at different temperatures of the stack ($T_{cond.}$ = 40°C, λ = 2.0, I = 305 A).

It can be seen that the membrane resistance of the cells increased at the front side of the stack as the stack temperature was raised from 62°C to 67.5°C; meanwhile the other membrane resistances remained the same.

At operating temperature of 70°C the measured membrane resistances of the other cells started to increase uniformly. This shows that the gradual drying of the cells has already started as the calculations in table 1 prove.

Table 1: Measured *(m)* and calculated *(c)* operating parameters (λ = 2.0, I = 300A) / $p_{cath.in}$ *(m* = 1094 ± 2 hPa, $p_{cath.out}$ *(m)* = 1037 ± 1 hPa

$T_{cath.in}$ *(m)* / °C	$rh_{cath.in}$ *(m)* / %	$rh_{cath.in}$ *(c)* / %	$T_{cath.out}$ *(m)* / °C	$rh_{cath.out}$ *(c)* / %
41.6	90	89.5	62	120
41.8	90	89.5	65	104.5
41.9	90	89.5	67.5	93.5
42.3	89.5	89.5	70	84
42.3	88.5	89.5	72.5	75.5

The highest increase of the membrane resistance can be observed close to the stack end-plates. According to this the water content of the border cells seem to be lower, which can be related to the thermal management of the fuel cell system. Consequently the optimal operating temperature at this operating point should be set at 65°C to 67.5°C.

During the experiments, the stack temperature was increased from 62°C to 72.5°C and the condensing temperature from 15°C to 40°C. Compared to the operation in closed loop configuration under manufacturer settings with a stoichiometric ratio of 2.0, the stack voltage was increased by rising the operating temperature from 39.0 V to 39.8 V at a nominal current of 300 A. This is equivalent to a performance gain of 240 W (2 %). In addition, the difference of the minimum and maximum cell voltage has been reduced (see Figure 7). Thus, the humidity and temperature distribution could be homogenized in the stack which also positively affects the dynamic power rating capability of the fuel cell.

5 Conclusions

This work presents a study of the cathode exhaust gas recirculation including an oxygen supply for a polymer electrolyte fuel cell stack to maintain a constant oxygen concentration at the cathode inlet. In closed loop configuration the operation does not depend on the ambient air and results in additional humidification of the cathode inlet gas.

The results of the theoretical analysis illustrate the correlation of the operation parameters temperature, pressure and cathodic stoichiometric ratio on the relative humidity of the cathode gas, which has a impact on the efficiency and durability of the PEMFC.

The relative humidity of the cathode gas is adjusted by variation of the operating temperatures and the stoichiometric ratio. The stack temperature and the cathode stoichiometric ratio have to be increased and the condenser temperature has to be decreased to avoid fuel cell flooding and vice versa to avoid membrane.

Additionally, the presented study focuses on the optimization of the fuel cells water management and hence its performance in closed loop configuration. The performance of the considered fuel cell system was enhanced by 2 % regarding the adjustment of the condenser and stack temperatures.

This work forms the basis for further investigations. As shown above, in a steady-state condition, the needed amount of injected oxygen does not depend on the stoichiometric ratio. Hence, the use of pure oxygen is to prefer in closed loop configuration to increase the oxygen partial pressure and thus the cell potential. Therefore, the oxygen concentration as well as the operating pressure should be increased. Both will influence the cell potential positively.

Especially the oxygen enrichment will reduce the concentration losses, which increases the efficiency and maximum power output of the stack [7, 9]. On the other hand, the raised oxygen content will have a negative influence on the degradation of the fuel cell (mainly carbon corrosion and oxygen reduction), which has to be taken into account [5].

Furthermore the oxygen enrichment opens the opportunity of an increase of the operating temperatures and pressure, which is an important factor in terms of the cooling system scaling.

Acknowledgments

The work presented is part of the research project „Fuel Cell and Hydrogen Systems - FUCHS“ (project number: 20Y1105B) supported by the Federal Ministry of Economic Affairs and Energy. The authors gratefully acknowledge the support received. In addition, the authors acknowledge the contribution of their colleagues Simon Coners, Gema Montaner Rios, Igor ySokolov and Claudia Werner.

List of Symbols

λ	Cathodic stoichiometric ratio
Cath.	Cathode
C_{O2}	Oxygen concentration / %
Cond.	Condenser
F	Faraday constant = 96485 C mol^{-1}
F_{O2}	Fractional oxygen concentration in dry gas phase
$H_2O(v)$	Water vapor
$H_2O(l)$	Liquid water
I	Electric stack current / A
n	Molar flow rate / mol s^{-1}
N_2	Nitrogen
O_2	Oxygen
T_0	Standard temperature = 298.15 K
T_{FC}	Stack temperature / K
p_0	Standard pressure = 101325 Pa
p_{abs}	Absolute pressure / Pa
$p_{cath.}$	Cathodic absolute pressure = 101325 Pa
p_s	Saturation vapor pressure / Pa
R	Universal gas constant = 8.314 J· mol^{-1} K^{-1}
rh	Relative humidity / %
v_0	Standard flow rate / m^3 s^{-1}
x_i	Mole fraction of component
Z	Number of cells = 60 (HyPM XR12); 40 (HyPM HD4)

Appendix

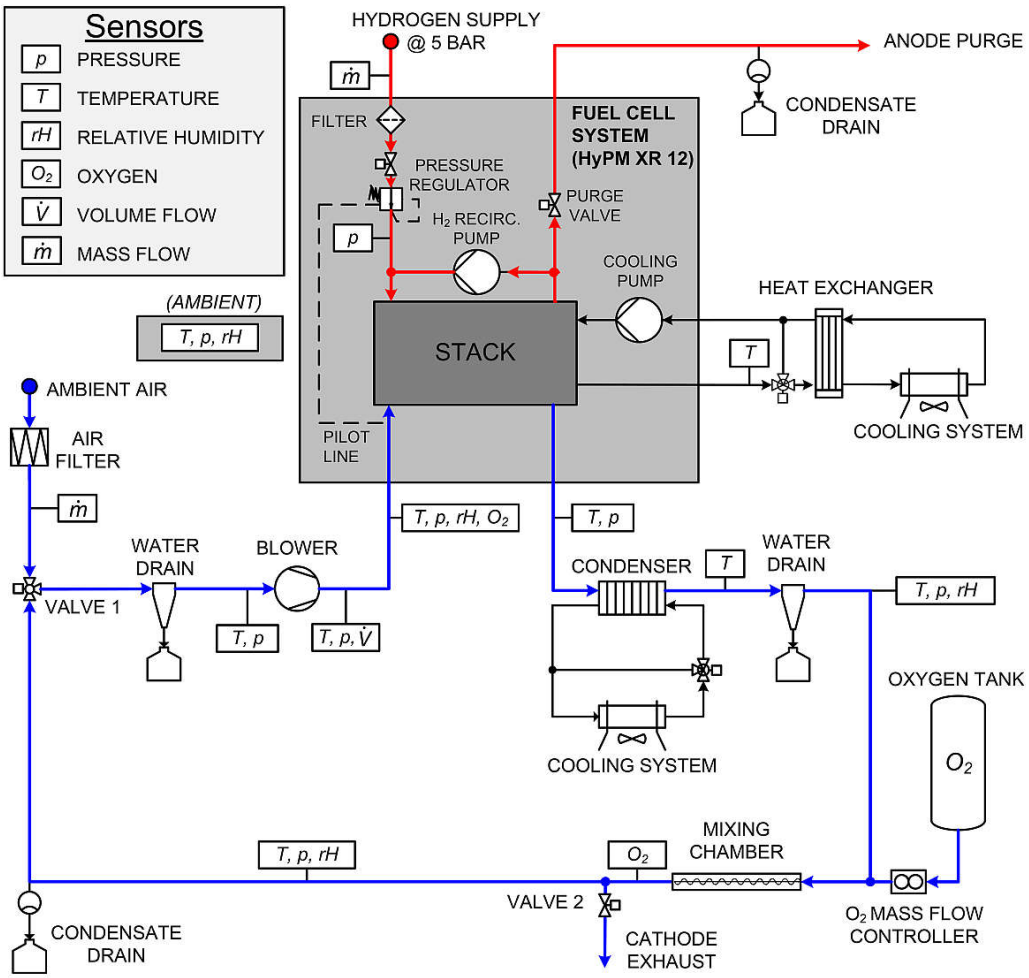

Fig. 9: Process scheme including the HyPM XR-12 PEMFC system

Table 2: Used components and sensors for the experimental setup

Component	**Typ**	**Manufacturer**
Fuel cell system	HyPM XR12	Hydrogenics
Blower	G-BH7	Gardener Denver
Vent 1 & 2	J3C	J+J
Condenser	Alfa Nova 27-20L	Alfa Laval
Water drain	AS 2	Mankenberg
Water trap	SN 2	Mankenberg

Sensors	**Typ**	**Manufaturer**	**Measuring range**	**Measurement error**
Oxygen	FOSPOR-T1000-TS-NEO	Ocean Optics	0…25 Vol.-% O_2	<5% m.v.
Relative humidity	AFK-E1	Kobold	0…100% rF	±(1,3+0,3 m.v.) % rF
Temperature	TMA H 644102XX4	Kobold	-200…+600 °C	<0,5% of full scale
Pressure	A -10	Wika	0-1,6 bar	<1% of full scale
Volume flow	Vortex DI 50	Höntzsch	2,8…212 m³/h (46,7…3533 slpm)	<1% m.v. + 0,3% of full scale
Impedance spectroscope	IM 6	Zahner	10 µHz to 8 MHz	< 0,0025%

References

[1] M. Ji, Z. Wei, Energies, **2009**, 2, pp. 1057-1106

[2] K. Jiao, X. Li, Progress in Energy and Combustion Science, **2011**, 37, pp. 221-291

[3] I. Tolj, D. Bezmalinovic, F. Barbir, International Journal of Hydrogen Energy **2011**, 36, 13106

[4] F. Nandjou, J.-P. Poirot-Crouvezier, M. Chandesris, J.-F. Blachot, C. Bonnaud, Y. Bultel, Journal of Power Sources, **2016**, 326, 183

[5] R. Borup, J. Meyers, B. Pivovar, Y. S. Kim, R. Mukundan, N. Garland, D. Myers, M. Wilson, F. Garzon, D. Wood, P. Zelenay, K. More, K. Stroh, T. Zawodzinski, J. Boncella, J. E. McGrath, M. Inaba, K. Miyatake, M. Hori, K. Ota, Z. Ogumi, S. Miyata, A. Nishikata, Z. Siroma, Y. Uchimoto, K. Yasuda, K. Kimijima, N. Iwashita, Chemical Reviews, **2007**, 107, 3937

[6] F. N. Büchi, S. Srinivasan, J. Electrochem. Soc. **1997**, 144, pp. 2767-2772

[7] F. Barbir, PEM Fuel Cells: Theory and Practice, Elsevier Inc., **2005**, pp. 305

[8] B. J. Kim, M. S. Kim, International Journal of Hydrogen Energy, **2012**, 37, 4290-4299

[9] J. Larminie, A.Dicks, Fuel Cell Systems Explained, 2nd Edition, Wiley, **2003**, pp. 83-84

[10] C. Werner , L. Busemeyer, J. Kallo, International Journal of Hydrogen Energy, **2015**, 40, 11595-11603

[11] HyPM XR 12 Installation and Operation Manual, Version 1.0, Hydrogenics Corp, **2007**

[12] W. Wagner, A. Pruß, J. Phys. Chem. Ref. Data, **2002**, 31, pp.486-494